Title

Flipping the Switch: Reverse-Demand Voltage-Sensitive Fluorophores

Journal

Journal of the American Chemical Society, 144(29)

ISSN

0002-7863

Authors

McCann, Jack T

Benlian, Brittany R

Yaeger-Weiss, Susanna K

et al.

Publication Date

2022-07-27

DOI

10.1021/jacs.2c05385

Peer reviewed

HHS Public Access

Author manuscript

J Am Chem Soc. Author manuscript; available in PMC 2023 July 27.

Published in final edited form as:

J Am Chem Soc. 2022 July 27; 144(29): 13050–13054. doi:10.1021/jacs.2c05385.

Flipping the switch: reverse-demand voltage-sensitive fluorophores

Jack T. McCann[‡], **Brittany R. Benlian**[§], **Susanna K. Yaeger-Weiss**[‡], **Isaac J. Knudson**[‡], **Minyi He**[‡], **Evan W. Miller**[‡,§,†,*]

[‡]Department of Chemistry, University of California, Berkeley, California 94720, United States.

[§]Department of Molecular & Cell Biology, University of California, Berkeley, California 94720, United States.

[†]Department of Helen Wills Neuroscience Institute, University of California, Berkeley, California 94720, United States.

Abstract

Fluorescence microscopy with fluorescent reporters that respond to environmental cues are a powerful method for interrogating biochemistry and biophysics in living systems. Photoinduced electron transfer (PeT) is commonly used as a trigger to modulate fluorescence in response to changes in the biological environment. PeT based indicators rely either on PeT into the excited state (acceptor PeT) or out of the excited state (donor PeT). Our group has been developing voltage-sensitive fluorophores (VF dyes) that respond to changes in biological membrane potential (V_m). We hypothesize that the mechanism of voltage sensitivity arises from acceptor PeT (a-PeT) from an electron-rich aniline-containing molecular wire into the excited state fluorophore, resulting in decreased fluorescence at negative V_m. Here we reverse the direction of electron flow to access donor-excited PeT (d-PeT) VF dyes by introducing electron-withdrawing (EWG), rather than electron-rich molecular wires. EWG-containing VF dyes show voltage-sensitive fluorescence, but with the opposite polarity: hyperpolarizing V_m now give fluorescence increases. We use a combination of computation and experiment to design and synthesize five d-PeT VF targets, two of which are voltage sensitive.

Graphical Abstract

[*]**Corresponding Author** evanwmiller@berkeley.edu.

Supporting Information. Experimental procedures, NMR spectra, and supporting figures. This material is available free of charge via the Internet at http://pubs.acs.org.

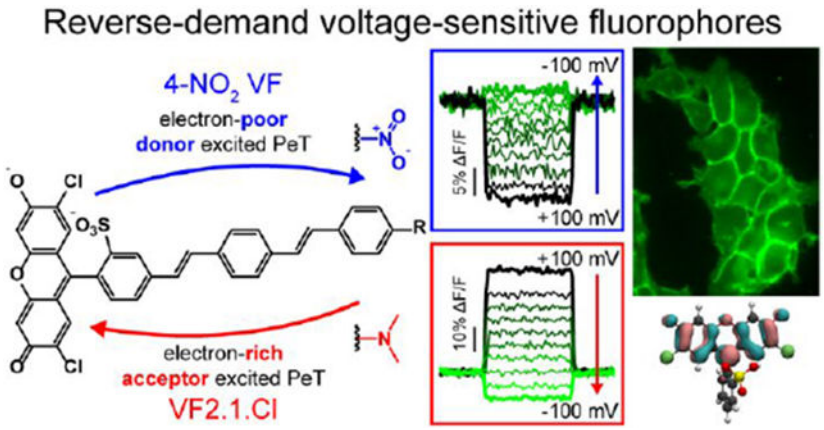

Biological membrane potentials (V_m) arise from differences in ion concentrations across a selectively-permeable lipid bilayer and are a defining feature of life.[1] Visualizing cellular V_m with fluorescent indicators offers a powerful complement to traditional electrode methods and seeks to address problems of low-throughput, poor spatial resolution, and invasiveness associated with electrophysiology.[2] Fluorescent dyes have long been used to monitor biologically relevant analytes, reactions, and properties. Modulating photoinduced electron transfer (PeT) is a powerful method for designing fluorescent reporters.[3-6] By controlling PeT into or out of the excited state of a fluorophore based on the binding or reaction withanalytes like ions[7-8] and reactive metabolites,[9-11] PeT provides a generalizable trigger for designing fluorescent reporters.

Our group has been exploring the application of PeT-based triggers for monitoring V_m.[12] We postulate that voltage sensitivity within Voltage-sensitive Fluorophores (or VF dyes) arises from a V_m-sensitive electron transfer (Scheme 1);[13-14] therefore, the direction of the electron transfer matters. At hyperpolarized V_m, the electron moves from a molecular wire buried in the plasma membrane into a fluorophore on the extracellular face PeT is occurring and the dye is dim. At depolarized V_m, the voltage decreases the rate of PeT, allowing fluorescence to occur, and the dye brightens. Consistent with this hypothesis, VF dyes possess fluorescence turn-on responses upon membrane depolarization,[12] nanosecond response kinetics,[15] and voltage-dependent fluorescence lifetimes.[16]

To date, all VF dyes make use of an aniline-containing molecular wire to achieve voltage sensitivity in an acceptor-PeT (a-PeT) configuration in which the fluorophore acts as the electron acceptor.

However, if the hypothesis about the mechanism of voltage sensing is correct, replacing the electron-rich aniline with an electron-withdrawing group (EWG) should decrease the frontier molecular orbital energies of the wire and enable donor-excited PeT (d-PeT) (Scheme 1, Figure 1a-b). In this configuration, hyperpolarized V_m decreases the rate of PeT. This results in fluorescence brightening at hyperpolarized potentials and would provide the first example of a molecular sensor architecture with bi-directional electron flow for sensing in a-PeT or d-PeT configurations.

Here we show that electron-poor molecular wires with EWG substituents can be incorporated into a VF dye scaffold, reversing the direction of electron flow, and inverting the sign of the fluorescence response to V_m changes. We calculate the HOMO/LUMO energies of a series of EWG-containing molecular wires, synthesize 5 new EWG-VF dyes, characterize their spectroscopic properties, and evaluate their voltage sensitivity in mammalian cells. Two of the new dyes show voltage sensitivity, but with an inverted polarity relative to previously reported aniline-containing VF dyes.[17-19]

To investigate the possibility of reversing the polarity of VF dyes through d-PeT, we performed DFT calculations to estimate the relative HOMO/LUMO energies of the orthogonal fluorophore and molecular wire systems. Complete EWG-VFs were modeled in two components, the fluorophore and the molecular wire (Figure 1c, d, S1). Geometries were optimized using def2-TZVP/ωB97XD, and calculated HOMO/LUMO values (Figure 1e) were normalized to a shared sulfonate orbital (Figure S2) to allow direct orbital energy comparison between molecules.[20-21] The HOMO/LUMO values calculated using the individual components gave values that matched well with those calculated using the entire VF dye (Figure S1). Component-based computationscut CPU time by nearly two-thirds and enable a mix-and-match comparison of fluorophores and molecular wires.

For aniline-substituted VF2.1.Cl,[17-19] the molecular wire and fluorophore HOMO is higher than the fluorophore HOMO, with a HOMO-HOMO (H-H) gap of approximately −0.05 eV, indicating the possibility of a-PeT (wire-to-fluorophore). Conversely, the molecular wire LUMO of VF2.1.Cl is higher than the LUMO of 2',7'-dichloro-3-sulfonofluorescein, with a LUMO-LUMO (L-L) gap of approximately +0.27 eV, indicating that d-PeT (fluorophore-to-wire) is unlikely for this molecule (Figure 1).

For EWG-VF dyes like 4-NO_2-VF, we find the complementary configuration: the wire LUMO of 4-NO_2-VF is lower than the fluorescein LUMO by −0.58 eV, indicating the possibility of d-PeT.[20] We calculated the orbital energies for other EWG-containing molecular wires, 2,4-diNO_2, 3-NO_2, 4-CN, and 4-SO_2Me (Scheme 2, Figure 1). Both 4-NO_2-VF and 2,4-diNO_2-VF possess L-L gaps of around −0.6 eV or larger. 3-NO_2-VF has an intermediate L-L gap value of −0.33 eV, while the L-L gaps for 4-CN-VF and 4-SO_2Me-VF decrease substantially to −0.18 and −0.07 eV, respectively (Figure 1, Table 1). For comparison, the L-L and H-H gaps for non-voltage sensitive VF2.0.Cl (4-H), are +0.12 eV and +0.61 eV, respectively. Based on these data, we hypothesize that strongly EWG substitutions, like 4-NO_2 and 2,4-diNO_2, might enable d-PeT VF dyes because of their large, negative L-L gaps.

To test the hypothesis that VF dyes could be “run in reverse”, we synthesized 5 different EWG-substituted stilbene derivatives. 4-NO_2, 3-NO_2, and 4-CN stilbenes could all be accessed via sequential Wittig/Heck/Wittig reactions, with the Wittig reactions carried out with K_2CO_3 as the base (Scheme S1). We synthesized 2,4-diNO_2 and 4-SO_2Me stilbene (**2b, 2e**) via a Horner-Wadsworth-Emmons reaction (Scheme S2), since we observed decomposition under Wittig conditions. Pd-catalyzed cross coupling of the EWG-substituted stilbenes (**2a-e**) with 5-bromo-2',7'-dichloro-3-sulfono-fluorescein (**1**) afforded EWG-VF dyes (**3a-e**).

All of the EWG-VF dyes display an invariant absorption maximum at 511 nm and emission maximum at 527 nm, owing to the common fluorophore (Figure 2). The molecular wire absorbance varies for EWG-VF dyes (Figure 2, Table 1). The quantum yield of fluorescence (Φ_{fl}) for EWG-VF dyes ranges from 0.09 to 0.71 (Table 1). Both 4-NO_2-VF and 2,4-diNO_2-VF have low Φ_{fl} values, indicating a high degree of PeT quenching. The pK_a values of the phenolic oxygen of fluorescein of the EWG-VF dyes range from 4.8 to 5.7 (Figure S3, Table S2). In the presence of high concentrations of thiols (2 mM glutathione), EWG-VFs display stability comparable to VF2.1.Cl ($p = 0.4$, Figure S4).

All of the EWG-VF dyes stain the plasma membranes of HEK293T cells (Figure 3a-f). Widefield epifluorescence microscopy reveals a “chicken-wire” pattern of cellular staining, indicating localization to the plasma membrane. 4-NO_2-VF has the brightest membrane staining, 2-fold brighter than VF2.1.Cl (Figure 3a, f, g, Table 1). We assessed the voltage sensitivity of the new, EWG-VF dyes in HEK293T cells using whole-cell patch clamp electrophysiology (Figure 4a-e). EWG-VF dyes with 4-nitro substituents show voltage sensitivity, but with a reverse polarity. Unlike VF2.1.Cl, which displays a fluorescence increase upon membrane depolarization, the fluorescence of 4-NO_2-VF and 2,4-diNO_2-VF decreases upon depolarization and becomes brighter upon hyperpolarization (Figure 4f).

Despite a higher nominal voltage sensitivity, 2,4-diNO_2-VF shows very low cellular fluorescence (Figure 3a, b, S5), ~40-folder lower than 4-NO_2-VF, making 4-NO_2-VF the most useful EWG-VF for cellular voltage imaging. 4-NO_2-VF is capable of monitoring evoked action potentials (APs) in cultured rat hippocampal neurons (Figure S6). In a single trial, 4-NO_2-VF reports on APs with an average $\Delta F/F$ of −1.3% (±0.14, $n = 17$, standard deviation) and a signal-to-noise ratio (SNR) of 9.1 (±1.0, $n = 17$). The response to neuronal AP depolarization is a fluorescence decrease, showing that d-PeT indicators function in complex cellular contexts.

At hyperpolarizing potentials more negative than −100 mV, 4-NO_2-VF becomes even brighter, achieving a turn on response for hyperpolarization of +2.4% (Figure 5a-b). At extreme hyperpolarized potentials, the optical response deviates from the linearity observed between −100 mV and +100 mV (Figure 5b). Hyperpolarized potentials play important roles in inhibitory neurotransmission and more broadly, in the physiology of mitochondria, where resting mitochondrial potentials are in the range of −100 to −200 mV.[22-23]

Finally, we show that 4-NO_2-VF can be used in simultaneous, two-color mapping of V_m dynamics along with a far-red voltage indicator, BeRST-1 (Figure 5c-e, S7).[24] 4-NO_2-VF exactly follows the time course of BeRST-1, indicating that the d-PeT method provides fast response kinetics and is compatible with two color imaging (Figure 5f).

In summary, we report the design, synthesis, and validation of d-PeT based VFs for voltage imaging. DFT was used to determine the orbital energies of molecular wires with EWGs and 2',7'-dichloro-3-sulfonofluorescein. Five d-PeT VFs were synthesized to test the computational method. Both 4-NO_2-VF and 2,4-diNO_2-VF are voltage sensitive, acting as turn-on indicators for hyperpolarization. While a-PeT and d-PeT have been used to design fluorescent reporters,[5] this is the first demonstration that HOMO/LUMO levels can

be tuned to access both a-PeT and d-PeT for detection of a biologically-relevant analyte with the same fluorophore scaffold. Future directions include improving voltage sensitivity by pairing electron-deficient molecular wires with electron-rich fluorophores and applying reverse VFs to biological contexts where the V_m polarity is switched compared to plasma membranes, for example in mitochondria[25] and organelles.[26]

Supplementary Material

Refer to Web version on PubMed Central for supplementary material.

ACKNOWLEDGMENT

E.W.M. acknowledges support from the Camille Dreyfus Foundation and NIH (R35GM119855). J.T.M., B.R.B., and I.J.K. were supported, in part, by a training grant from NIH (T32GM066698). S.K.Y.-W. was supported, in part, by a training grant from NIH (T32GM008295). We thank Dr. Hasan Celik and the staff of the College of Chemistry NMR facility for their assistance. Instruments in CoC-NMR are supported in part by NIH S10OD024998. 900MHz NMR supported by NIH GM68933. We thank Drs. Kathleen Durkin and Dave Small for their assistance with computations. The CoC-MGCF is supported by NIH S10OD023532.

REFERENCES

1. Kandel ER; Schwartz JH; Jessell TM; Siegelbaum SA; Hudspeth AJ; Mack S, Principles of neural science. 5th ed. ed.; McGraw-Hill Education LLC: New York, N.Y, 2013.
2. Peterka DS; Takahashi H; Yuste R, Imaging voltage in neurons. Neuron 2011, 69 (1), 9–21. [PubMed: 21220095]
3. de Silva PA; Gunaratne NHQ; McCoy CP, A molecular photoionic AND gate based on fluorescent signalling. Nature 1993, 364 (6432), 42–44.
4. Daly B; Ling J; de Silva AP, Current developments in fluorescent PET (photoinduced electron transfer) sensors and switches. Chemical Society Reviews 2015, 44 (13), 4203–4211. [PubMed: 25695939]
5. Nagano T, Development of fluorescent probes for bioimaging applications. Proc Jpn Acad Ser B Phys Biol Sci 2010, 86 (8), 837–847.
6. Lavis LD, Teaching Old Dyes New Tricks: Biological Probes Built from Fluoresceins and Rhodamines. Annual Review of Biochemistry 2017, 86 (1), 825–843.
7. Minta A; Kao JPY; Tsien RY, Fluorescent indicators for cytosolic calcium based on rhodamine and fluorescein chromophores. Journal of Biological Chemistry 1989, 264 (14), 8171–8178. [PubMed: 2498308]
8. Burdette SC; Walkup GK; Spingler B; Tsien RY; Lippard SJ, Fluorescent Sensors for Zn2+ Based on a Fluorescein Platform: Synthesis, Properties and Intracellular Distribution. Journal of the American Chemical Society 2001, 123 (32), 7831–7841. [PubMed: 11493056]
9. Kojima H; Nakatsubo N; Kikuchi K; Kawahara S; Kirino Y; Nagoshi H; Hirata Y; Nagano T, Detection and Imaging of Nitric Oxide with Novel Fluorescent Indicators: Diaminofluoresceins. Analytical Chemistry 1998, 70 (13), 2446–2453. [PubMed: 9666719]
10. Tanaka K; Miura T; Umezawa N; Urano Y; Kikuchi K; Higuchi T; Nagano T, Rational Design of Fluorescein-Based Fluorescence Probes. Mechanism-Based Design of a Maximum Fluorescence Probe for Singlet Oxygen. Journal of the American Chemical Society 2001, 123 (11), 2530–2536. [PubMed: 11456921]
11. Ueno T; Urano Y; Setsukinai K.-i.; Takakusa H; Kojima H; Kikuchi K; Ohkubo K; Fukuzumi S; Nagano T, Rational Principles for Modulating Fluorescence Properties of Fluorescein. Journal of the American Chemical Society 2004, 126 (43), 14079–14085. [PubMed: 15506772]
12. Liu P; Miller EW, Electrophysiology, Unplugged: Imaging Membrane Potential with Fluorescent Indicators. Accounts of Chemical Research 2020, 53 (1), 11–19. [PubMed: 31834772]

13. de Silva AP; Gunaratne HQN; Habib-Jiwan J-L; McCoy CP; Rice TE; Soumillion J-P, New Fluorescent Model Compounds for the Study of Photoinduced Electron Transfer: The Influence of a Molecular Electric Field in the Excited State. Angewandte Chemie International Edition in English 1995, 34 (16), 1728–1731.

14. Li L.-s., Fluorescence Probes for Membrane Potentials Based on Mesoscopic Electron Transfer. Nano Letters 2007, 7 (10), 2981–2986. [PubMed: 17880257]

15. Beier HT; Roth CC; Bixler JN; Sedelnikova AV; Ibey BL, Visualization of Dynamic Sub-microsecond Changes in Membrane Potential. Biophysical Journal 2019, 116 (1), 120–126. [PubMed: 30579565]

16. Lazzari-Dean JR; Gest AMM; Miller EW, Optical estimation of absolute membrane potential using fluorescence lifetime imaging. eLife 2019, 8, e44522. [PubMed: 31545164]

17. Boggess SC; Lazzari-Dean JR; Raliski BK; Mun DM; Li AY; Turnbull JL; Miller EW, Fluorescence lifetime predicts performance of voltage sensitive fluorophores in cardiomyocytes and neurons. RSC Chemical Biology 2021, 2 (1), 248–258. [PubMed: 34212146]

18. Woodford CR; Frady EP; Smith RS; Morey B; Canzi G; Palida SF; Araneda RC; Kristan WB; Kubiak CP; Miller EW; Tsien RY, Improved PeT Molecules for Optically Sensing Voltage in Neurons. Journal of the American Chemical Society 2015, 137 (5), 1817–1824. [PubMed: 25584688]

19. Miller EW; Lin JY; Frady EP; Steinbach PA; Kristan WB; Tsien RY, Optically monitoring voltage in neurons by photoinduced electron transfer through molecular wires. Proceedings of the National Academy of Sciences 2012, 109 (6), 2114–2119.

20. Chi W; Chen J; Liu W; Wang C; Qi Q; Qiao Q; Tan TM; Xiong K; Liu X; Kang K; Chang Y-T; Xu Z; Liu X, A General Descriptor ΔE Enables the Quantitative Development of Luminescent Materials Based on Photoinduced Electron Transfer. Journal of the American Chemical Society 2020, 142 (14), 6777–6785. [PubMed: 32182060]

21. Turnbull JL; Benlian BR; Golden RP; Miller EW, Phosphonofluoresceins: Synthesis, Spectroscopy, and Applications. Journal of the American Chemical Society 2021, 143 (16), 6194–6201. [PubMed: 33797899]

22. Alpert NM; Guehl N; Ptaszek L; Pelletier-Galarneau M; Ruskin J; Mansour MC; Wooten D; Ma C;Takahashi K; Zhou Y; Shoup TM; Normandin MD; El Fakhri G, Quantitative in vivo mapping of myocardial mitochondrial membrane potential. PLOS ONE 2018, 13 (1), e0190968. [PubMed: 29338024]

23. Gerencser AA; Chinopoulos C; Birket MJ; Jastroch M; Vitelli C; Nicholls DG; Brand MD, Quantitative measurement of mitochondrial membrane potential in cultured cells: calcium-induced de- and hyperpolarization of neuronal mitochondria. The Journal of physiology 2012, 590 (12), 2845–71. [PubMed: 22495585]

24. Huang Y-L; Walker AS; Miller EW, A Photostable Silicon Rhodamine Platform for Optical Voltage Sensing. Journal of the American Chemical Society 2015, 137 (33), 10767–10776. [PubMed: 26237573]

25. Klier PEZ; Martin JG; Miller EW, Imaging Reversible Mitochondrial Membrane Potential Dynamics with a Masked Rhodamine Voltage Reporter. J Am Chem Soc 2021, 143 (11), 4095–4099. [PubMed: 33710896]

26. Saminathan A; Devany J; Veetil AT; Suresh B; Pillai KS; Schwake M; Krishnan Y, A DNA-based voltmeter for organelles. Nature Nanotechnology 2021, 16 (1), 96–103.

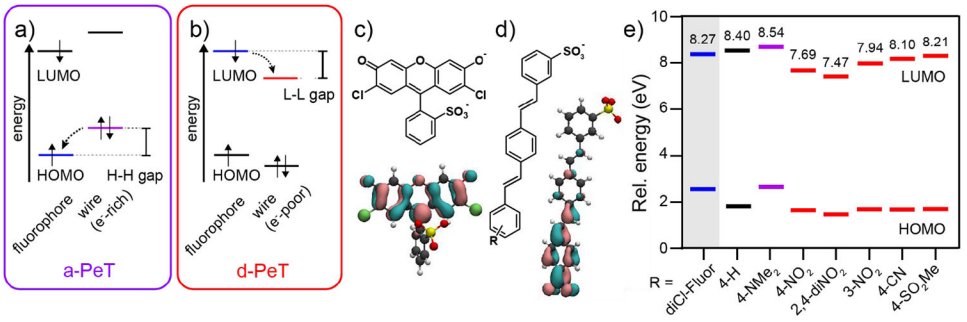

Figure 1.

Controlling photoinduced electron transfer processes in voltage-sensitive fluorophores. Frontier molecular orbital diagrams for fluorescein and either **a)** electron-rich molecular wires that exhibit acceptor-excited PeT (a-PeT) or **b)** electron-poor molecular wires that exhibit donor-excited PeT (d-PeT). c) Structure and LUMO of 2',7'-dichloro-3-sulfonofluorescein. **d)** Structure and LUMO of variousmolecular wires. This specific example is 4-NO_2-VF, but R can equal any of the substituents indicated in panel (e). **e)** Plot of calculated energy levels (eV) of 2',7'-dichloro-3-sulfonofluorescein and various molecular wires with the indicated R group.

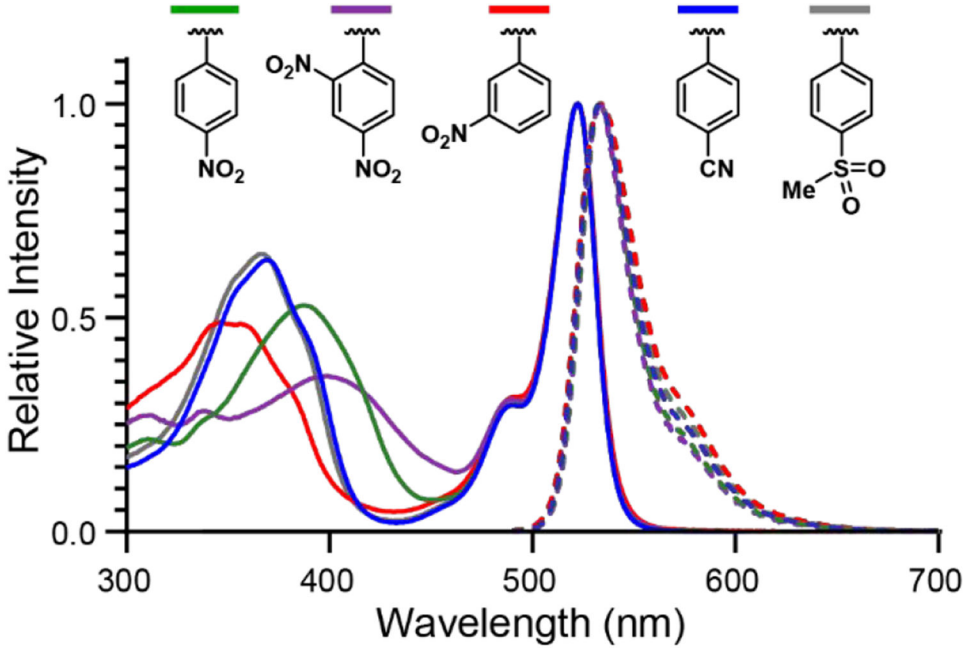

Figure 2.

UV-vis and emission spectra of reverse VF dyes. Plot of relative intensity vs wavelength for reverse VF dyes. Absorbance is shown in solid lines; emission is shown in dashed lines. Spectra are normalized to the λ_{max} and acquired with 1.25 μM dye in 0.1M KOH in EtOH. Excitation provided at 480 nm.

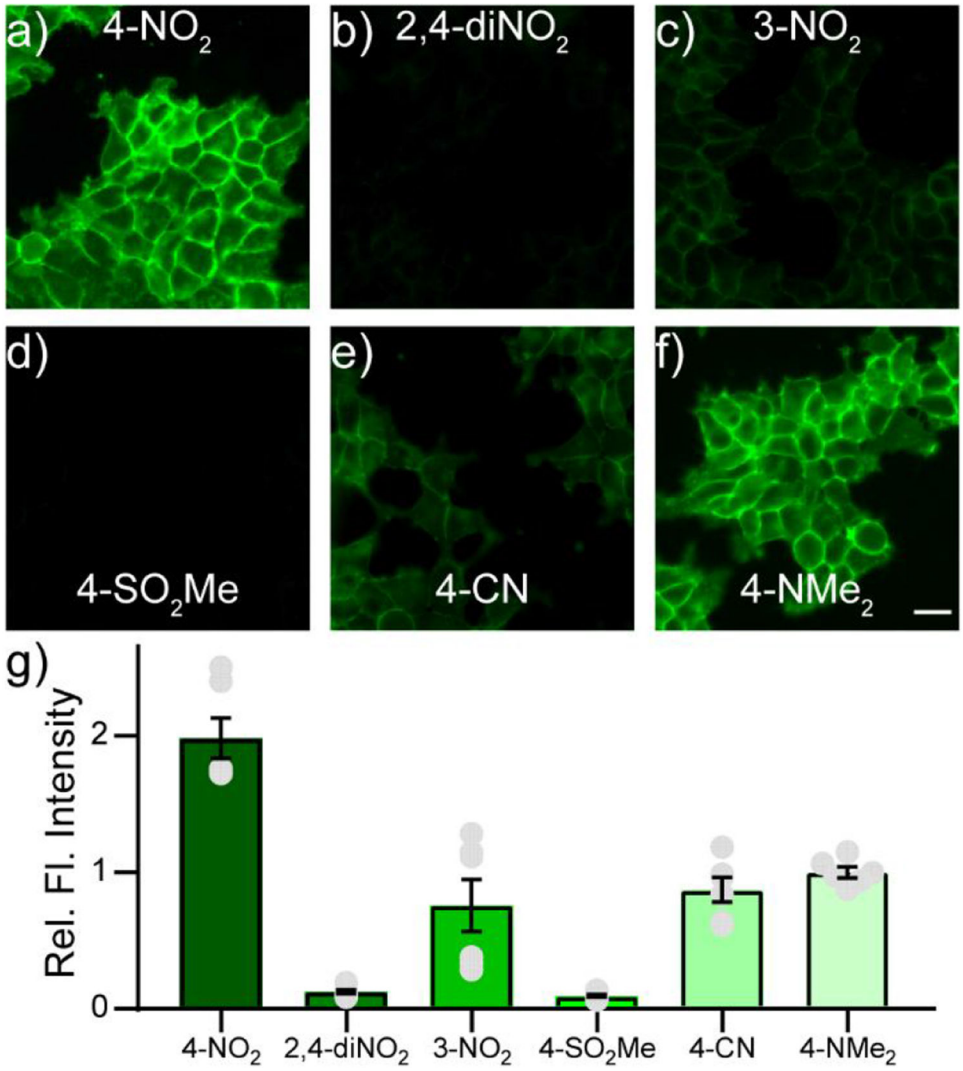

Figure 3.

Live cell imaging with reverse VF dyes. Widefield epifluorescence images of HEK293T cells treated with either **a)** 4-NO_2-VF **(6), b)** 2,4-diNO_2-VF **(13), c)** 3-NO_2-VF **(17), d)** 4-SO_2Me-VF **(23), e)** 4-CN-VF (**27**), or **f)** VF2.1.Cl (4-NMe_2). All dyes were loaded at 250 nM. Scale bar is 20 μm. **g)** Plot of cellular fluorescence intensity of HEK293T cells loaded with the indicated dye. Data are mean ± S.E.M. for n = 6 independent experiments. For each experiment, or coverslip, we analyzed between 80 – 100 cells and took the mean fluorescence intensity.

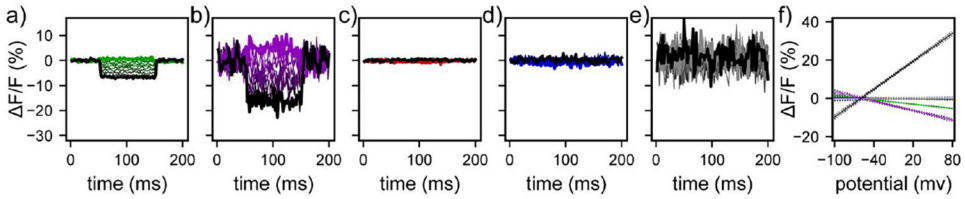

Figure 4.

Voltage sensitivity of EWG-containing VF dyes in living cells. Plots of ΔF/F vs time for HEK293T cells loaded with either **a)** 4-NO_2-VF, **b)** 2,4-diNO_2-VF, **c)** 3-NO_2-VF, **d)** 4-CN-VF, or **e)** 4-SO_2Me-VF. Cells were held at −60 mV under whole-cell voltage-clamp conditions and then stepped to potentials ranging from −100 mV to −100 mV in 20 mV increments. **f)** Plot of ΔF/F per 100 mV vs V_m (in mV) for 4-NO_2-VF (green, n= 8), 2,4-diNO_2-VF (magenta, n = 5), 3-NO_2-VF (red, n = 5), 4-CN-VF (blue, n = 3), 4-SO_2Me-VF (gray, n = 4), or VF2.1.Cl (black). Data are mean ± S.E.M. VF2.1.Cl data is from Turnbull, *et al.*[21]

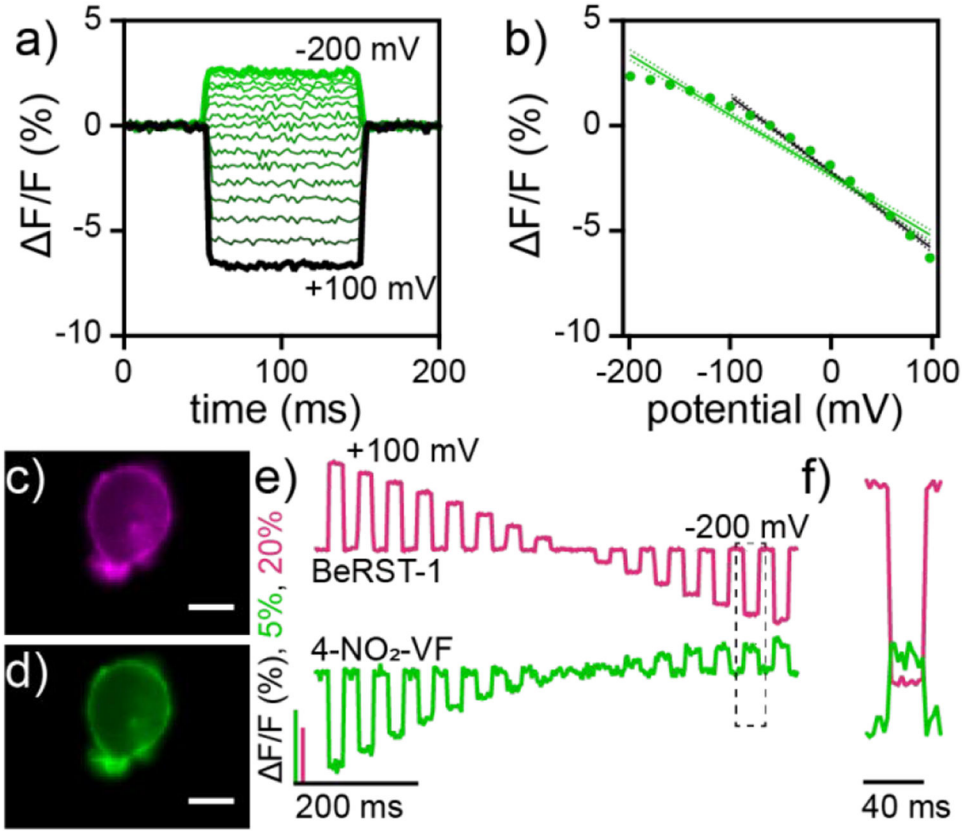

Figure 5.

Voltage sensitivity of 4-NO_2-VF at hyperpolarized potentials. **a)** Plot of ΔF/F vs time for HEK293T cells loaded with 4-NO_2-VF. Cells were held at −60 mV under whole-cell voltage-clamp conditions and stepped to potentials ranging from +100 mV to −200 mV in 20 mV increments. **b)** Plot of ΔF/F vs V_m (in mV) for 4-NO_2-VF. Data are mean ± SEM for n = 5 cells. Fluorescence images of a HEK cell stained with **c)** BeRST-1 and **d)** 4-NO_2-VF. **e)** Plot of ΔF/F vs time for the same cell imaged with both BeRST and 4-NO_2-VF. **f)** Zoomed-in region of e.

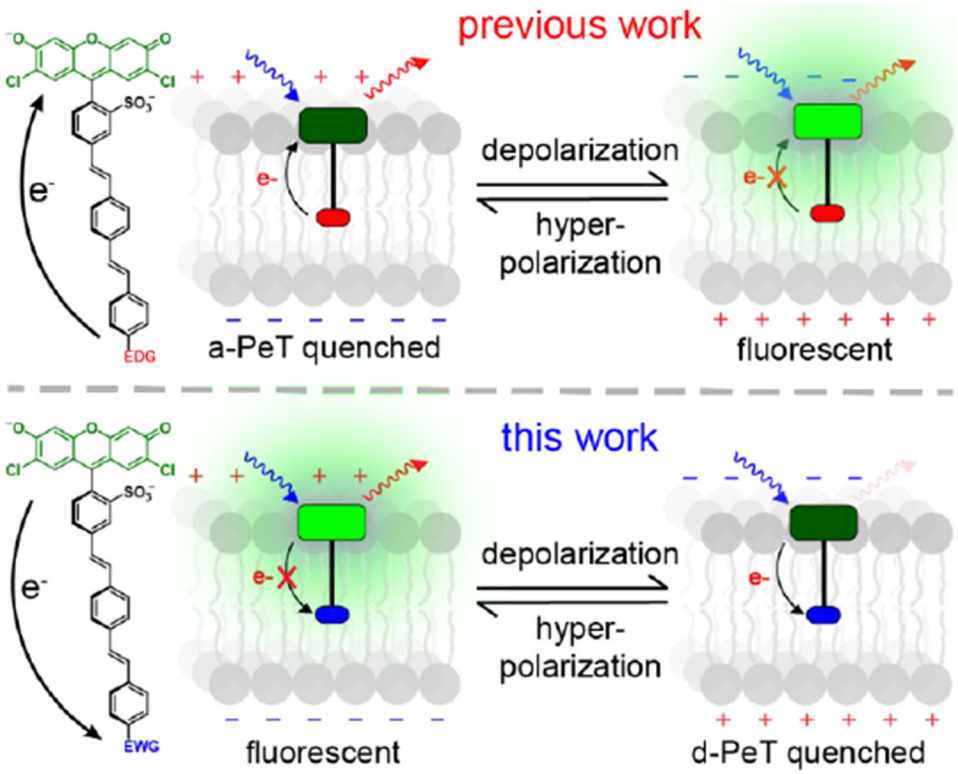

Scheme 1.
PeT in Voltage-sensitive Fluorophores (VF) dyes

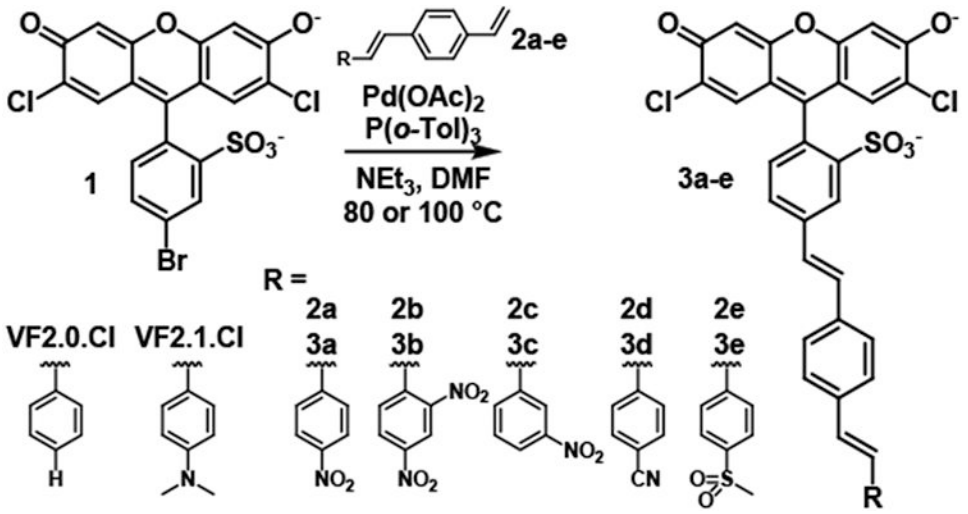

Scheme 2.
Synthesis of EWG-containing VF dyes

Table 1.

Properties of EWG-VFs

Compound	R	ΔF/F[a]	LUMO (eV)[b]	L-L Gap (eV)[c]	λ_{abs}[d] (nm)	Rel. Cell Brightness[e]	Φ_{fl}[f]
3a	4-NO_2	−3.8 ± 0.1	7.69	−0.58	387	2.0 ± 0.1	0.23
3b	2,4-diNO_2	−8.2 ± 0.7	7.45	−0.79	397	0.13 ± 0.02	0.10
3c	3-NO_2	−0.4 ± 0.01	7.94	−0.33	342	0.76 ± 0.2	0.71
3d	4-CN	−0.4 ± 0.1	8.09	−0.18	366	0.87 ± 0.1	0.71
3e	4-SO_2Me	0 ± 0.7	8.21	−0.07	360	0.095 ± 0.01	0.51
VF2.1.Cl	4-NMe_2	25 ± 1	8.54	+0.27	389[g]	1.0 ± 0.04	0.12[g]
VF2.0.Cl	H	0	8.40	+0.12	360[g]	---	0.83[g]

[a] per 100 mV in HEK293T cells.

[b] Values normalized to respective sulfonate orbital.

[c] Difference between LUMO of 2',7'-dichloro-3-sulfonofluorescein and corresponding molecular wire.

[d] For molecular wire; acquired in 0.1 M EtOH-KOH.

[e] Determined in HEK293T cells; all values relative to brightness of VF2.1.Cl.

[f] Determined in EtOH-KOH.

[g] Values from Boggess, *et al.*[17]